Mineralogical Magazine, December 2006, Vol. 70(6), pp. 669–687

Contrasts in gem corundum characteristics, eastern Australian basaltic fields: trace elements, fluid/melt inclusions and oxygen isotopes

KHIN ZAW[1,*], F. L. SUTHERLAND[2], F. DELLAPASQUA[1], C. G. RYAN[3], TZEN-FU YUI[4], T. P. MERNAGH[5] AND D. DUNCAN[6]

[1] CODES ARC Centre of Excellence in Ore Deposits, University of Tasmania, Private Bag 79, Hobart, Tasmania 7001, Australia
[2] Mineralogy, Australian Museum, 6 College Street, Sydney, NSW 2010, Australia
[3] CSIRO Exploration and Mining, School of Physics, University of Melbourne, VIC 3010, Australia
[4] Institute of Earth Science, Academica Sinica, Taipei, Taiwan
[5] Australian Geological Survey Organization, Canberra, ACT 2601, Australia
[6] McPherson Duncan & Associates, 18 Old Summerleas Road, Kinston, Tasmania 7050, Australia

ABSTRACT

Corundum xenocrysts from alkaline basalt fields differ in characteristics and hence lithospheric origins. Trace element, fluid/melt inclusion and oxygen isotope studies on two eastern Australian corundum deposits are compared to consider their origins. Sapphires from Weldborough, NE Tasmania, are magmatic (high-Ga, av. 200 ppm) and dominated by Fe (av. 3300 ppm) and variable Ti (av. 400 ppm) as chromophores. They contain Cl, Fe, Ga, Ti and CO_2-rich fluid inclusions and give $\delta^{18}O$ values (5.1−6.2‰) of mantle range. Geochronology on companion zircons suggests several sources (from 290 Ma to 47 Ma) were disrupted by basaltic melts (47 ± 0.6 Ma). Gem corundums from Barrington, New South Wales, also include magmatic sapphires (Ga av. 170 ppm; $\delta^{18}O$ 4.6−5.8‰), but with more Fe (av. 9000 ppm) and less Ti (av. 300 ppm) as chromophores. Zircon dating suggests that gem formation preceded and was overlapped by Cenozoic basaltic melt generation (59−4 Ma). In contrast, a metamorphic sapphire-ruby suite (low-Ga, av. 30 ppm) here incorporates greater Cr into the chromophores (up to 2250 ppm). Fluid inclusions are CO_2-poor, but melt inclusions suggest some alkaline melt interaction. The $\delta^{18}O$ values (5.1−6.2‰) overlap magmatic sapphire values. Interactions at contact zones (T = 780−940ºC) between earlier Permian ultramafic bodies and later alkaline fluid activity may explain the formation of rubies.

KEYWORDS: Gem corundum, trace elements, fluid/melt inclusions, oxygen isotopes, basalts, mantle, eastern Australia.

Introduction

EASTERN Australia contains a major Mesozoic–Cenozoic basaltic belt, notable for numerous scattered gem corundum deposits within many of its alkali basaltic lava fields (Oakes *et al*., 1996; Sutherland, 1996). The corundums are largely concentrated in alluvial deposits, as xenocrysts released from the pyroclastic, volcaniclastic and solid lava basaltic hosts, and some fields have supported or still support mining and secondary treatment ventures (Coldham, 2003). The origins of these gem corundums from deep-seated sources, formed prior to basaltic transport, have had considerable debate, based on their gemmological characteristics, trace element geochemistry, mineral inclusions, isotopes and geochronological relationships with the host basalts (see Sutherland and Schwarz, 2001). As yet, only limited data are available on fluid and

* E-mail: Khin.Zaw@utas.edu.au
DOI: 10.1180/0026461067060356

melt inclusions and oxygen isotope values for eastern Australian corundums, to define their sources prior to their delivery as xenocrysts or rarely in xenoliths.

The origins involved in eastern Australian gem corundum suites represent part of a wider, global picture for such basaltic gem associations (Upton *et al*., 1999; Garnier *et al*., 2004), particularly for the concentrations noted along the Western Pacific continental margins, including those from Australia, South East Asia, eastern China and eastern Russia (Sutherland *et al*., 2004*a*). A large literature invokes a range of potential lithospheric origins for many of these eastern deposits (e.g. Guo *et al*., 1996; Limtrakun *et al*., 2001; Sutthirat *et al*., 2001; Vysotskii *et al*., 2002; Sutherland *et al*. 2002*a*,*b*, 2003; Saminpanya *et al*., 2003; Yui *et al*., 2003; Garnier *et al*., 2004).

In this paper, we present trace element chemistry, fluid/melt inclusion characteristics and oxygen isotope compositions of corundums from two gem deposits in eastern Australia, from basalt fields in northeastern Tasmania and eastern New South Wales. The results are used to constrain likely conditions of contrasting corundum genesis.

Geological setting

The two gem corundum deposits studied here (Fig. 1) are linked to Cenozoic basaltic fields that erupted through granite-intruded Palaeozoic to Early Mesozoic fold belts. The 450–350 Ma Lachlan Orogen underlies the Weldborough field in northeastern Tasmania, and the 300–200 Ma New England Orogen underpins the Barrington field in eastern New South Wales (Veevers, 2001). The alkali basalts that furnished the gem corundums as xenocrysts also released zircon xenocrysts. The latter mineral helps to date gem source formation (U-Pb dating) and the subsequent magmatic transport of this material (fission track dating), which is supplemented by radiometric dating of host basalts (see Sutherland and Fanning, 2001).

Weldborough sapphire field

The sapphires form rounded alluvial grains and broken fragments of etched 'dogstooth' prisms and rhombohedral crystals; they reach up to 264 (53 g) carats and reportedly up to 900 carats (180 g) in size and include 'star' stones (Bottrill, 1996). The general geology in relation to the alluvial sample sites (Fig. 2) is characterized by Devonian granitoids, Early Devonian Mathinna beds, Permian and Cenozoic sedimentary beds and Cenozoic basalt flows of two ages (46 Ma and 16 Ma). The main sapphire concentrations occur in the Weld River; here its catchment 6 km SE of Weldborough drains a 47 Ma sequence of coarse basaltic agglomerates and capping basalt flows up to 230 m thick, before discharging northwards into the Ringarooma River basin (McClenaghan *et al*., 1982; Yim *et al*., 1985; Sutherland and Wellman, 1986; Moore, 1991). An isolated gem-bearing,

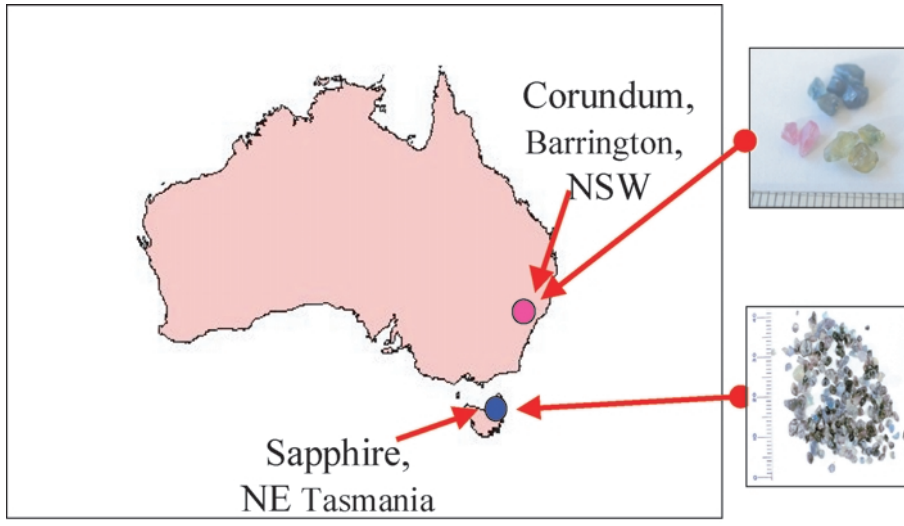

FIG. 1. Map of Australia showing the locations of the NE Tasmania and Barrington gemfields.

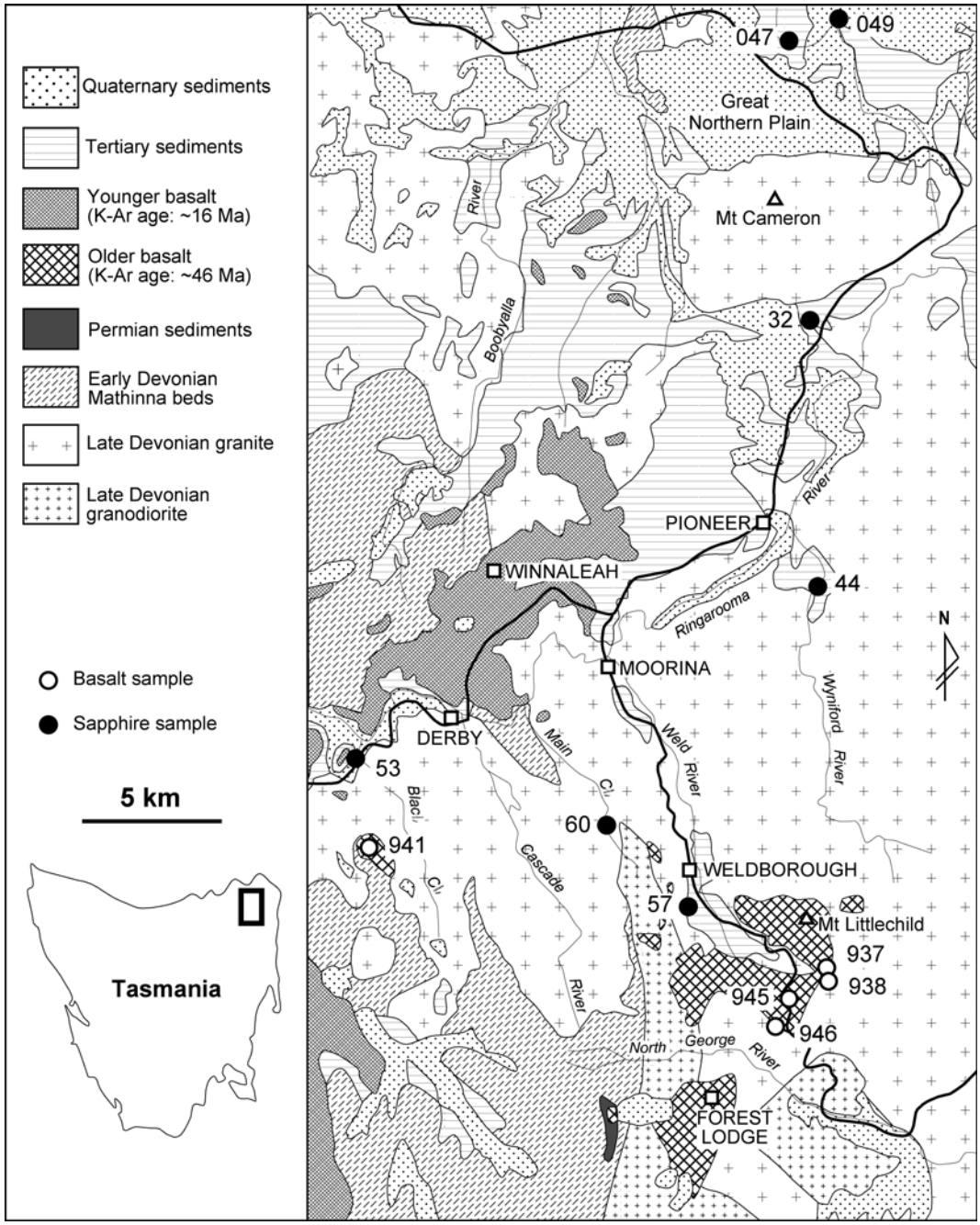

FIG. 2. Geological map of NE Tasmania showing basalt areas, sampling sites and corundum/zircon localities (inset).

sub-basaltic placer at Gray's Hill, 12 km E of Weldborough was included in this study. Previous geochemical data on the Weldborough and Gray's Hill basalts (McClenaghan *et al*., 1982; Sutherland *et al*., 2004*b*) are supplemented by new analyses in this study.

Barrington sapphire-ruby field

Sapphires and rubies here form rounded and broken, magmatically corroded crystals, some retaining fusion crusts, and occur in the soils and alluvial deposits shed from the 59–4 Ma basalt sequence (Sutherland and Graham, 2003; Roberts *et al*., 2004). The blue, green and yellow sapphire crystals range to >12 carats (2.4 g), while pink and red crystals range to >19 carats (4 g) in size (P. Kennewell, Cluff Resources Pacific P.L., pers. comm., 2005). The corundums and associated zircons are found throughout the basalt plateau drainage over a 300 km^2 area, but are particularly concentrated in alluvial terrace, mass wastage and recent gravel deposits of the Upper Manning River (Gummi Flats), the site studied here. The alkali basalts in the Barrington sequence have been analysed extensively (see O'Reilly and Zhang, 1995; Sutherland and Fanning, 2001) and no further analyses were made in this study.

Analytical methods

Corundum trace element analyses

Eleven blue and green sapphires from the northeastern Tasmanian sample were analysed at the CODES ARC Centre of Excellence in Ore Deposits of the University of Tasmania. The polished, mounted grains were analysed in both core and rim positions, under standard procedures using a New Wave UP-213 Nd: YAG Q-switched Laser Ablation System coupled with an Agilent HP 4500 Quadrupole ICP-MS (Sarah Gilbert, analyst). The international standard NIST 612 was used as the primary standard to calculate concentrations and correct for ablation depth, and the basaltic glass BCR-2 was used as the secondary standard. Only Ti, V, Cr, Fe and Ga were found in measurable amounts. A further run also analysed for Be, Nb, Ta and Sn in the core regions.

Twenty sapphires and rubies from an earlier study (Sutherland *et al*., 1998*a*) from the Gummi, Barrington field were analysed at the Particle-induced X-ray emission (PIXE) facility at the University of Guelph, Canada (Campbell and Czamanske, 1998). Each polished corundum wafer was analysed in two or more spots (Mary Garland, analyst). The PIXE data were processed by GUPIX software (using steel alloy standards and synthetic corundum as an internal check), as described by Maxwell *et al.* (1995).

Fluid/melt inclusion analyses

The petrography of fluid/melt inclusions in the corundums was investigated initially at CODES, University of Tasmania. Laser Raman microprobe analysis was undertaken at the Australian Geological Survey Organisation, Canberra, using a Dilor® SuperLabram spectrometer equipped with a holographic notch filter, 600 and 1800 g/mm gratings, and a liquid-N_2-cooled, 2000×450 pixel CCD detector. The inclusions were illuminated with 514.5 nm laser excitation from a Spectra Physics model 2017 argon ion laser, using 5 mW powers on the samples, and a single 30 s accumulation. The focused laser spot on the samples was ~1 μm in diameter. Wavenumbers are accurate to ± 1 cm^{-1} as determined by plasma and neon emission lines. For the analysis of CO_2, O_2, N_2, H_2S and CH_4 in the vapour phase, spectra were recorded from 1000 to 3800 cm^{-1} using a single 20 s integration time per spectrum. Raman detection limits are estimated to be ~0.1 mol.% for CO_2, O_2 and N_2, and 0.03 mol.% for H_2S and CH_4, and errors in the calculated gas ratios are generally <1 mol.%.

A PIXE study, at CSIRO Exploration and Mining, Sydney, imaged selected melt and fluid inclusions in the corundum (Fig. 4); a raster-scanned beam of 3 MeV protons was focused into a beam-spot of ~1.5 μm using the CSIRO-GEMOC Nuclear Microprobe (Ryan *et al.,* 1995, 2002). This approach was used to determined the composition of the original trapped fluid and led to a standardless measure of inclusions compositions (Tables 3 and 4). This approach was also used to image inclusions content (Fig. 5).

Corundum oxygen isotope analyses

The analyses used the CO_2 laser-fluorination method (Sharp, 1990). The Weldborough sapphires were analysed at the Institute of Earth Science Laboratories, Taipei, Taiwan, employing a Finnegan MAT 252 mass spectrometer to analyse CO_2 gas (Tzen-Fu Yui, analyst). The results are given as per mil $\delta^{18}O$ relative to Mean Standard Ocean Water (MSOW), have an analytical precision of ±0.1‰, and were normalized using a UWG-2 garnet standard with $\delta^{18}O$ of +5.8‰ (Yui *et al.*, 2003). The Barrington corundums were analysed at the Isotope Geoscience Unit, East Kilbride, Scotland, using a VG PRISM 3 dual inlet isotope ratio mass

spectrometer and the methodology detailed by Giuliani *et al.* (2005). Precision and accuracy on quartz standards were ±0.1‰ (1σ) and results are reported relative to V-SMOW (Vienna standard mean ocean water).

Zircon geochronology

Zircon fission track dating was carried out on three types of zircon megacrysts from the sub-basaltic placer below Gray's Hill by Geotrack International P.L. The analyses used similar methods and statistical treatments to those reported for zircon megacrysts from the Barrington basaltic gemfields (see Sutherland and Fanning, 2001; Roberts *et al*., 2004).

Reconnaissance Sensitive High-Resolution Ion Micro-Probe (SHRIMP) data on Weldborough zircon megacrysts are reported here from unpublished SHRIMP I analyses (P.D. Kinny and F.L. Sutherland, analysts). The method employed to calculate the young U-Pb isotope dates is detailed by Coenraads *et al*. (1990). This dating used zircons previously studied for fission track dating (Yim *et al.,* 1985), but also used other zircon megacrysts from the Weldborough basalt plateau (Thomas Plains) and the Gray's Hill sub-basaltic placer.

Basalt whole-rock analyses

Representative samples of Weldborough basalts were crushed and analysed by standard XRF techniques, at the SES-CODES laboratory, University of Tasmania. Each sample was ground in a tungsten carbide mill and analysed using fusion discs of the powdered material. The trace element arrays were determined from pressed pills using an Au X-ray tube and a ScMo X-ray tube (Phil Robinson and Katie McGoldrick, analysts).

Results

Trace elements

In Weldborough sapphires (Table 1), Fe is dominant (1929−4425 ppm), Ti is subordinate and highly variable (5−2277 ppm) and Cr (0.1−17 ppm) and V (0.5−11 ppm) are low, while Ga levels are significant (104−520 ppm). There is more Fe in cores than in rims (272−535 ppm or 9−23% more), as is the case for Ti (2−437 ppm or 2−80% more), except for one grain (no. 3), with a Ti-depleted core (46 ppm, i.e. 60% less). The cores are also enriched in Ga (4−39 ppm, or 2−17% more). Plots of Fe_2O_3/TiO_2 *vs.* Cr_2O_3/Ga_2O_3 (Fig. 3) fall well within ratios for magmatic corundums (Sutherland *et al*., 1998*a*).

Barrington corundums (Table 2) fall into a higher-Ga suite (64−299 ppm) and a lower-Ga suite (15−52 ppm). The higher-Ga suite resembles the Weldborough sapphires, in terms of the dominance of Fe (5780−13325 ppm) over highly variable Ti (51−1242 ppm). The Fe contents within individual grains range from 140 to 1054 ppm (i.e. by 1−25%), while Ti contents

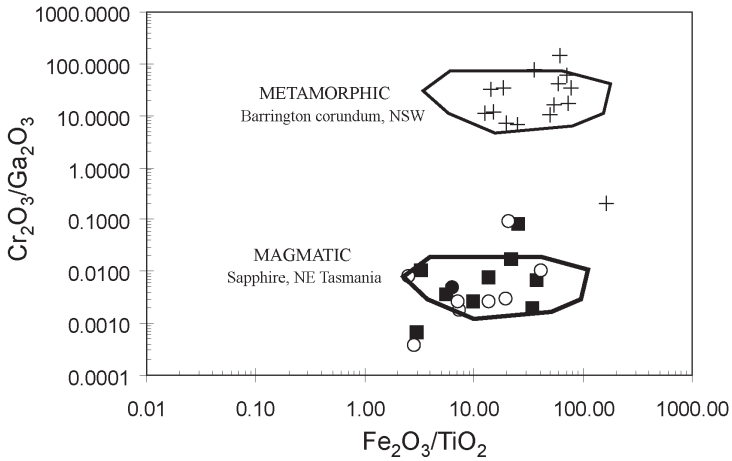

FIG. 3. Cr_2O_3/Ga_2O_3 *vs*. Fe_2O_3/TiO_2 plot of NE Tasmanian sapphires and Barrington corundums. Barrington metamorphic corundums (crosses); NE Tasmanian sapphires, (solid squares – cores; circles – rims). Note that because they are below the Cr detection limit, the Barrington magmatic sapphires would plot just under the 0.0001 vertical axis value, between 1 and 14 on the horizontal axis.

TABLE 1. Trace element LA ICP-MS analyses (ppm) of sapphires from NE Tasmania.

Grain no (site)	Fe range (av.)	Ti range (av.)	V range (av.)	Cr range (av.)	Ga range (av.)
2 (rim)	2669–3171 (2920)	69–156 (113)	8.3–9.3 (8.8)	1.9–2.9 (2.4)	161–162 (162)
2 (core)	3255–3654 (3455)	146–154 (150)	10.0–11.5 (10.7)	0.6–0.3 (0.4)	169–194 (181)
Total grain	(3188)	(132)	(9.8)	(1.4)	(172)
3 (rim)	3007–3406 (3207)	427–482 (455)	1.2–1.3 (1.3)	0.8–0.31 (0.6)	201–202 (202)
3 (core)	3406–3689 (3548)	404–414 (409)	1.7–1.5 (1.6)	0.4–0.3 (0.3)	225–240 (236)
Total grain	(2378)	(432)	(1.4)	(0.5)	(224)
4 (rim)	2875–3070 (2973)	63–85 (74)	1.0–1.0 (1.0)	0.4–0.2 (0.3)	188–199 (194)
4 (core)	2836–3654 (3245)	164–238 (201)	0.9–1.3 (1.1)	0.2–0.7 (0.5)	201–237 (219)
Total grain	2836–3654 (3109)	63–238 (138)	(1.0)	(0.4)	(207)
6 (rim)	2781–2990 (2891)	16–314 (180)	1.2–1.5 (1.3)	0.9–0.5 (0.7)	104–112 (108)
6 (core)	3169–3223 (3196)	374–477 (423)	1.5–1.5 (1.5)	0.3–0.5 (0.4)	111–113 (112)
Total grain	(3044)	(302)	(1.4)	(0.5)	(110)
7 (rim)	3701–3900 (3801)	171–1780 (976)	6.0–5.1 (5.5)	1.6–1.7 (1.7)	191–207 (199)
7 (core)	3941–4307 (4124)	548–2277(1413)	7.9–8.6 (8.3)	1.6–1.2 (1.4)	200–221 (211)
Total grain	(3963)	(1195)	(6.9)	(1.5)	(205)
8 (rim)	1929–2215 (2072)	90–263 (177)	0.5–1.3 (0.9)	0.3–0.3 (0.3)	144–184 (164)
8 (core)	2487–2625 (2556)	273–347 (310)	0.7–0.6 (0.7)	0.4–0.3 (0.4)	171–174 (173)
Total grain	(2314)	90–347 (244)	(0.8)	(0.4)	(169)
9 (rim)	3075–3654 (3365)	5–220 (113)	2.7–1.6 (2.2)	5.1–25.4 (15.2)	194–264 (229)
9 (core)	3480–3939 (3710)	74–234 (154)	2.6–2.5 (2.6)	16.4–17.4 (16.9)	226–241 (234)
Total grain	(3508)	(134)	(2.4)	(16.1)	(232)
10 (rim)	2536–2849 (2693)	241–1267 (754)	2.3–4.6 (3.4)	0.3–0.2 (0.3)	468–481 (475)
10 (core)	2159–3409 (3284)	844–1101 (973)	4.6–4.5 (5.6)	0.1–0.2 (0.2)	507–520 (514)
Total grain	(2989)	(864)	(4.0)	(0.2)	(495)
11 (rim)	3669–3843 (3756)	80–92 (86)	3.7–3.6 (3.6)	1.3–0.5 (0.9)	165–169 (167)
11 (core)	4203–4425 (4214)	82–94 (88)	4.3–5.5 (4.9)	1.3–1.7 (1.5)	186–187 (187)
Total grain	(4035)	(82)	(4.1)	(1.2)	(177)
Total (n = 19)	1929–4425 (3284)	5–2272 (392)	0.4–11.5 (3.5)	1.0–25.4 (2.5)	104–520 (201)

Rims and cores represent two analyses of each, except grain 6 (rim) with three analyses. Results are standardized against Al content of 529,227 ppm for corundum. Laser ICP-MS Analyst: S. Gilbert.
Detection limit ranges (DL, ppm), with analytical precisions if >DL (% 1 standard deviation), for these elements are: Fe (2.11–3.62), ±1.7–2.1; Ti (0.22–0.61), ±1.8–3.9; V (0.02–0.03), ±1.7–4.8; Cr (0.34–0.57), ±2.6–35.8; Ga (0.02–0.04), ±1.4–3.2.

differ by 11–761 ppm (i.e. by 16–380%). The Cr contents mostly lie below detection limits (2–4 ppm) and V contents are <70 ppm. The Ga levels vary slightly within grains (1–71 ppm, i.e. by differences of 1–36%). The Ga levels and plots of Fe_2O_3/TiO_2 *vs.* Cr_2O_3/Ga_2O_3 match those of magmatic corundums (Saminpanya *et al.*, 2003). Comparisons of sapphires of 'magmatic' origin from Weldborough and Barrington show the average Fe content for Weldborough is 5634 ppm (or 170%) less, but the average Ti is 94 ppm (or 24%) greater, than the Barrington averages.

The lower-Ga Barrington suite, excluding the colourless crystal, notably has a greater concentration of Cr than in the 'magmatic' sapphire suites. The Cr systematically increases through the brown-, lavender- and purple-coloured corundums (av. 188–359 ppm) to reach the largest contents in pink-, purple-pink- and red-coloured corundums (323–2222 ppm). The Fe and Ti contents are variable through this colour range, but their average values are consistently smaller than in the Barrington 'magmatic' range, by 4620 ppm of Fe (52% less) and by 158 ppm of Ti

TABLE 2. Trace element PIXE analyses (ppm) of Barrington gem corundums, New South Wales.

Grain no. colour	Fe range (av.)	Ti range (av.)	Cr range (av.)	Ga range (av.)	V range (av.)
High-Ga suite (Ga >60 ppm)					
02 blue-green	5780–6160 (5920)	212–245 (229)	n.d.	64–65 (65)	45–69 (57)
13 green-blue	6105–7610 (6858)	62–183 (123)	n.d.	128–142 (135)	n.d.
11 dark blue	8462–9536 (8999)	75–361 (218)	n.d.	220–299 (260)	12–14 (13)
14 blue-green	9925–10065 (9995)	51–62 (57)	n.d.	259–261 (260)	7–9 (8)
12 blue-yellow	12308–13325(12817)	481–1242 (862)	n.d.	109–110 (110)	24–31 (28)
Total (n = 5)	5780–13325 (8918)	51–1242 (298)	n.d.	64–299 (166)	n.d.–69 (21)
Low-Ga suite (Ga <60ppm)					
01 colourless	3027–3045 (3036)	15–16 (16)	n.d.–7 (3)	19–20 (20)	n.d.–18 (9)
05 pink-brown	3720–3838 (3779)	64–65 (65)	248–258 (253)	26–27 (27)	25–26 (26)
06 lavender	5383–5607 (5495)	175–193 (184)	180–195 (188)	29–30 (30)	53–59 (56)
10 lavender	4990–5063 (5027)	207–214 (211)	315–322 (319)	44–47 (46)	95–97 (96)
20 grey lavender	5570–5607 (5589)	84–89 (87)	355–363 (359)	23–25 (24)	27–29 (28)
17 purple	3765–3827 (3796)	42–46 (44)	165–480 (323)	22–25 (24)	12–14 (13)
03 light purple	5610–5660 (5635)	292–326 (309)	490–500 (495)	45–46 (46)	154–162 (156)
15 violet	5660–5811 (5736)	365–387 (376)	499–501 (500)	48–49 (48)	194–195 (195)
04 purple pink	4416–4426 (4421)	256–258 (257)	946–961 (954)	33–34 (33)	18–18 (18)
07 pink	2859–3104 (2982)	29–37 (33)	688–730 (709)	22–23 (23)	15–15 (15)
08 bright pink	2565–2607 (2586)	30–30 (30)	907–951 (929)	15–18 (17)	16–17 (16)
18 bright pink	3074–3125 (3100)	43–44 (44)	722–763 (743)	20–20 (20)	13–14 (13)
16 bright pink	7543–7576 (7560)	338–346 (342)	1444–1683 (1564)	46–52 (49)	93–93 (93)
19 bright red	2529–2558 (2544)	57–60 (59)	1575–1629 (1602)	22–25 (24)	16–16 (16)
09 red	2986–3190 (3088)	41–46 (43)	2191–2253 (2222)	16–18 (19)	12–14 (13)
Total (n = 15)	2529–7576 (4292)	28–387 (140)	0–2253 (744)	15–52 (30)	n.d.–93 (51)

Ranges represent two analyses of each grain. Errors (ppm) for Fe are ±4 for 2500–3100 ppm, ±5 for 3100–4500 ppm, ±6 for 4500–7500 ppm, ±7 for 7500–9000 ppm, ±8 for 9000–12000 ppm, ±9 for > 12000 ppm. Errors (ppm) for Ti are ±2 for 15–250 ppm, ±3 for 250–500 ppm and ±4 for >500ppm. Errors (ppm) for Cr are ±1 for < 100 ppm, ±2 for 100–900 ppm, ±3 for 900–2000 ppm, ±4 for > 2000 ppm. Errors for Ga are ±1 for < 100 ppm, ±2 for < 100 ppm. Errors for V are ±2 for < 190, ±3 for 190–250 ppm.
n.d.: not detected.
PIXE analyst: M. Garland

(53% less). V is usually <100 ppm, but in some violet, purple and orange corundums lies between 150 and 200 ppm. The Ga levels and plots of Fe_2O_3/TiO_2 *vs.* Cr_2O_3/Ga_2O_3 (Fig. 3) place the lower-Ga Barrington suite within typical metamorphic corundum fields (Saminpanya *et al.*, 2003).

Composition of fluid/melt inclusions

The petrography of the fluid/melt inclusions indicates that they are from 10 to 50 μm in size (Fig. 4). Both fluid and melt inclusions appear in the same samples. Those in the Weldborough sapphires are mostly negative to rectangular in shape (Fig. 4*a*,*b*), whereas those in the Barrington corundums are elongated to elliptical form (Fig. 4*c*,*d*). Some inclusions are large enough to do PIXE analysis (in order to obtain their chemical composition), as for two fluid inclusions from the Weldborough sapphires and two melt inclusions from the Barrington corundums. The Weldborough analyses (Table 3) indicate that the dominant elements are Cl (15.3–16.6 wt.%), Fe (10.0–18.0 wt.%), Ga (0.6–1.1 wt.%) and Ti (0.27–0.81 wt.%) with Ca, K, Mn, Zn and other elements mostly below detection limits. Laser Raman spectroscopic (LRS) results indicate that the Cl-rich fluid is accompanied by the presence of CO_2.

Fluid/melt inclusions suitable for study were rare in the Barrington corundums studied here, but a few suitable melt inclusions were found in the low-Ga suite in a lavender corundum (Cobar 10) and in a pink corundum (Cobar 7). The PIXE probe results of melt inclusions in the Cobar 10

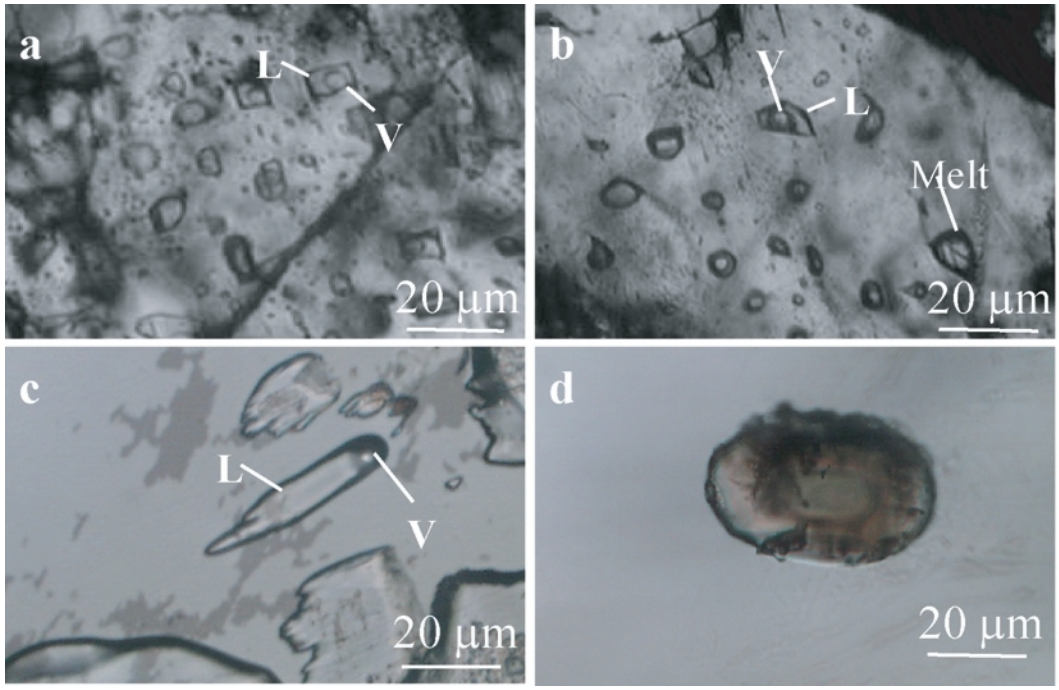

FIG. 4. Photomicrographs showing the characterisics of fluid/melt inclusions. (*a*) Fluid inclusions in Weldborough sapphire, NE Tasmania. (*b*) Fluid and melt inclusions in Weldborough sapphire, NE Tasmania. (*c*) A fluid inclusion in Barrington corundum, New South Wales. (*d*) A melt inclusion in Barrington corundum, New South Wales. V = Vapour, L = liquid.

showed high Cl (3.6–5.9 wt.%), K (1.4–4.5 wt.%), Fe (5.3–6.1 wt.%), Ca (0.3–0.4 wt.%), Ti (0.15–0.17 wt.%), Cr (0.23–0.28 wt.%), V (0.06–0.07 wt.%) and Ga (0.045–0.050 wt.%) (Table 4). The PIXE imaging of a melt inclusion in the lavender corundum also showed enrichments of the K and Cl, with minor Ca, Zn and Cu and depletion in Ti and V compared to the host corundum (Fig. 5).

The LRS analysis of the fluid inclusions in the Barrington samples indicated the presence of weak CO_2 bands at 1282 and 1387 cm^{-1} in the pink corundum, but no CO_2 bands in the lavender corundum. The LRS analysis of melt inclusions in the lavender corundum showed several weak bands below 600 cm^{-1}. Bands at 396 and 416 cm^{-1} are related to the host corundum, while bands at 227, 449, 570, 522 and

TABLE 3. PIXE analysis of element values (ppm) in fluid inclusions, Weldborough sapphire (Grain 3,6).

Main elements	Cl	Fe	Ga	Ti
Range	152829, 169089	100603, 180628	5593, 11256	2734, 8118
Error (wt.%)	±2.3%, ±2.6%	±0.5%, ±0.7%	±2.9%, ±3.4%	±3.8%, ±5.3%
Minor elements	**Ca**	**K**	**Mn**	**Zn**
Range	1286, 2465	863, 2241	174, 567	177, 371
Error (wt.%)	±12.2%, ±13.5%	±17.6%, ±26.4%	±30.9%, ±35.1%	±32.3%, ±33.9%

TABLE 4. PIXE analysis of element values (ppm) in melt inclusions in corundum from Barrington, New South Wales (Cobar, Grain 5,6).

Main elements	Cl	Fe	Ga	Ti	V
Range	35510, 59100	52900, 61200	450, 495	1500, 1700	574, 702
Error (ppm)	±991, ±997	±102, ±195	±18, ±34	±29, ±54	±23, ±43
Minor elements	**Ca**	**K**	**Cr**	**Zn**	**Cu**
Range	3400, 4300	1400, 45000	2300, 2800	272, 719	364, 188
Error (ppm)	±61, ±106	±180, ±254	±26, ±50	±14, ±37	±15, ±23

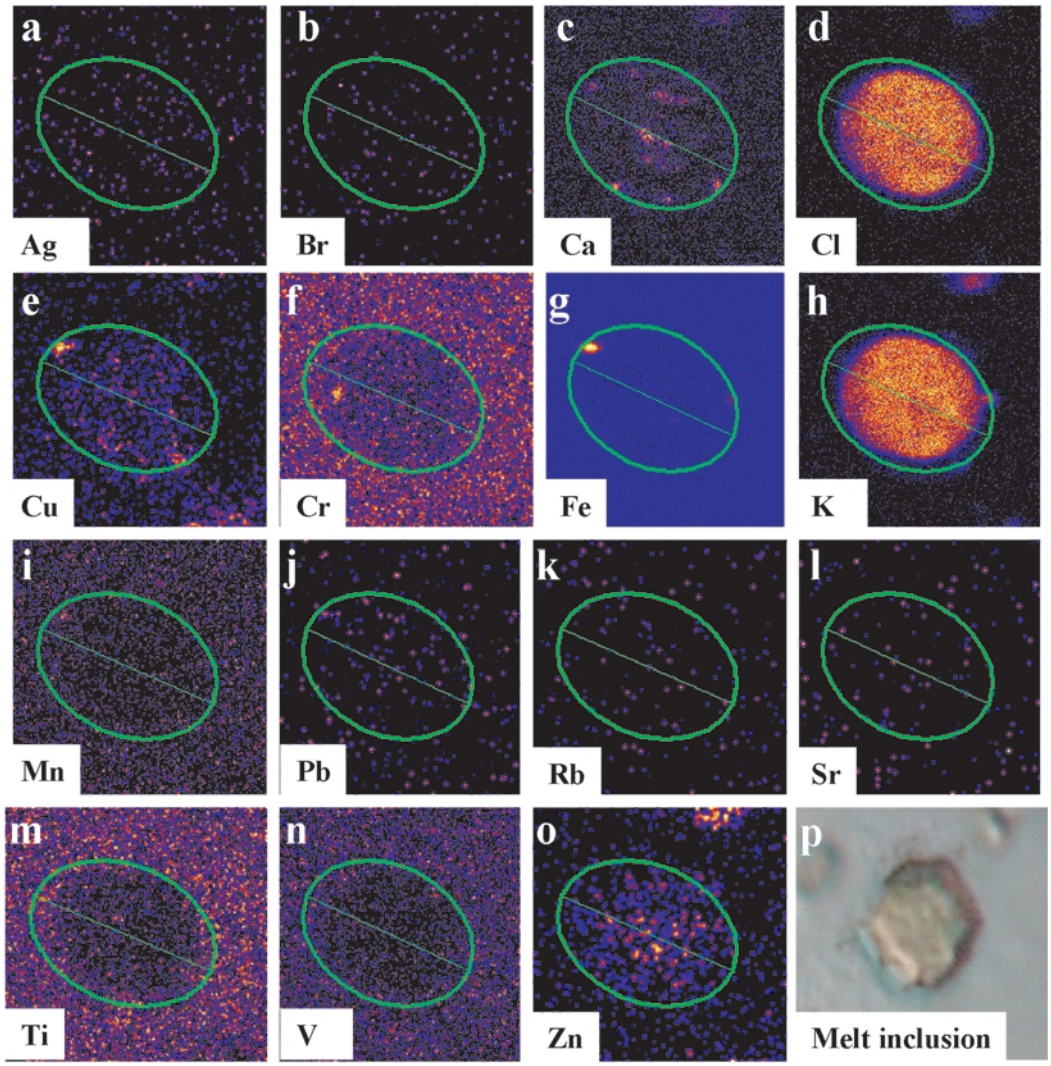

FIG. 5. PIXE images showing the elemental concentrations of a melt inclusion in Barrington corundum. Note enrichment of K and Cl.

TABLE 5. Oxygen isotope values (‰) for Weldborough sapphires, NE Tasmania.

Sample no.	Sample weight (mg)	Colour	$\delta^{18}O$ (‰)
1	75	Blue	6.1
2	59	Blue	5.2±0.1(2)
3	52	Blue	5.9
4	40	Blue	5.8±0.1(2)
5	93	Blue	5.5
6	269	Blue	4.1±0(2)
7	62	Blue	4.6±0.1(2)
8	343	Blue	5.4±0.1(2)
9	30	Blue	5.5
10	133	White	5.0
11	28	Blue	6.0
12	123	White	5.0±0.2(3)

574 cm^{-1} are related to a glassy silicate melt of a composition similar to that of plagioclase feldspar.

Corundum oxygen isotope results

Laser ablation $\delta^{18}O$ values for ten blue and two white Weldborough sapphires range from 4.6 to 6.0‰ (Table 5), values that largely overlap the range for corundums associated with mantle ultramafic host lithologies (up to + 5.5‰; Yui *et al.*, 2003; Giuliani *et al*., 2005). The $\delta^{18}O$ values across the colour range in the two Barrington corundum suites are listed in Table 6. The higher-Ga 'magmatic' suite types range from 4.6 to 5.8‰, which closely matches the Weldborough 'magmatic' suite sapphires. In comparison, the lower-Ga metamorphic suite types show a slightly higher range (5.1−6.2‰), and there is considerable overlap with 'magmatic' suites between 5.1 and 5.8‰. The highest value of 6.2‰ is for an orange corundum, that may in fact be a pale pink corundum stained by Fe oxide within microfractures (Roberts *et al*., 2004), so this may be an oxidized rather than a pristine isotope value.

Zircon geochronology

The fission track data from Gray's Hill (Table 7) suggests three zircon megacryst re-setting (eruptive) events at ~42, 53 and 71 Ma, with each group having distinctive ranges in colour and U content. The 42 and 53 Ma age zircons are almost within 2σ errors of each other and give an average fission track age of 47 Ma, close to the Weldborough zircon fission track ages. The observation of different U contents at different ages, however, suggests that separate zircon events were involved. This is supported by the U-Pb isotope dating of the F.T.-dated zircons, which also provides three separate formation ages (Table 4). The Gray's Hill F.T. data allows the possibility of an even younger basalt capping this site (<42 Ma) than those that occur on the Weldborough plateau (46−47 Ma; Sutherland and Wellman, 1986).

The U-Pb isotope data on the zircons from Weldborough Plateau and Gray's Hill areas (Table 8) suggest that multiple ages of zircon formation took place well before basaltic eruption reset the zircons between 42 and 72 Ma (Table 8), i.e. between 146±13 Ma to 290±25 Ma. Similar reconnaissance U-Pb dating on the actual zircons used in F.T. dating of downstream alluvial grains (Mutual Mine, Weld River; 46−47 Ma) by Yim *et al*. (1985) gave ages of 208±10, 211±11, 216±10, 223±9, 236±11 Ma, av. 219±10 Ma (F.L. Sutherland and P.D. Kinny, unpublished data). These results may incorporate partial resetting effects from heating as well as multiple formation ages, but are too imprecise to distinguish between the various possibilities. More refined SHRIMP II dating is in progress to test the alternatives.

Basalt host geochemistry

Analyses of representative basalts (Table 9) indicate the presence of primitive basanite (Mg no. ~0.71, An% 61, D.I. 27), slightly evolved alkali olivine basalt (Mg no. ~0.63, An% 48,

TABLE 6. Oxygen isotope values (‰) for Barrington corundums, New South Wales.

High-Ga Suite					Low-Ga Suite						
Black (opaque)	Blue (dark)	Blue (pale)	Green	Yellow	White (clear)	Pink (pale)	Pink (light)	Pink (dark)	Purple (dark)	Red (ruby)	Orange (oxidized)
4.6	5.2	5.2	5.4	5.8	5.5	5.4	5.4	5.1	5.8	5.9	6.2

TABLE 7. Zircon fission dating track summary, Gray's Hill gem-bearing deposit, NE Tasmania.

Colour set/ Grains (no.)	Ns range (av.)	Ni range (av.)	Na range (av.)	U range (av.) ppm	RHOs (av.) $\times 10^6$	RHOi (av.) $\times 10^6$	Age, Ma $\pm 2\sigma$
Set A: Pale to colourless rounded grains							
1–5	59–87	50–104	100	33–69	0.938–1.382	0.795–1.653	52.6
(5)	(78)	(83)	(100)	(55)	(1.236)	(1.313)	±5.6
Set B: Pale yellow-brown grains							
6–10	26–202	23–160	100	15–106	0.413–3.210	0.366–2.542	71.3
(5)	(72)	(56)	(100)	(37)	(1.138)	(0.890)	±8.4
Set C: Orange-brown grains							
10–15	97–164	127–269	50–100	84–249	1.541–5.212	2.018–5.975	41.9
(5)	(137)	(179)	(70)	(170)	(3.046)	(4.068)	±3.4

Pooled ages, calculated using a zeta of 87.7 ± 0.75 for U3 glass.
$RHO_D = 1.279 (\times 10^6)$ cm^{-2}
ND = 2012
Analyst: P.F. Green,
Geotrack International Report # 169, June 1989, Australian Museum, unpublished.

D.I. 31) and evolved hawaiite (Mg no. ~0.59, An% 39, D.I. 49). The basanites are sodic (Na_2O/K_2O ~2.3), the alkali basalt is intermediate (Na_2O/K_2O ~2), and the hawaiites are K-rich (Na_2O/K_2O ~1.7) in alkaline character.

Compatible trace element values are highest in the basanite (Ni + Cr ~800 ppm), moderately depleted in the alkali basalt (Ni + Cr ~400 ppm) and more depleted in the hawaiites (Ni + Cr ~350 ppm). Incompatible elements for these basalts are relatively enriched in Ba, Sr and Rb, particularly in the evolved alkali basalt and hawaiites (Ba 7500, Sr > 1100, Rb > 30 ppm), while Zr, Nb, La, Ce and Nd also increase towards the most evolved members (Zr from 205 to 479 ppm, Nb 52 → 101, La 39 → 63, Ce 69 → 113, Nd 31 → 45 ppm). Key element ratios for selected incompatible elements (Table 10) mostly lie within or close to the spectrum of ratios shown by HIMU-related Ocean Island Basalt (OIB) lavas, in which Large Ion Lithophile elements (LILE) are enriched, (Lanyon *et al*., 1993; Crawford *et al*., 1997). This is less evident in alkali basalt (AOB I), which shows greater La/Nb, Ba/Nb and Ba/Th than the typical limits for Tasmanian seamount HIMU-plume related basalts; this suggests that other mantle sources also contributed to the Weldborough basalt spectrum. A previously analysed Weldborough alkali basalt (AOB II), however, typifies the HIMU-related ratios observed in most Weldborough basalts (Sutherland *et al*., 2004*b*).

When normalized to primitive mantle values (Fig. 6) the new Weldborough basalts analyses all show enriched incompatible element patterns; the greatest enrichments appear in the evolved hawaiites, particularly in Zr, but accompany some relative depletion in Ti and Y during

TABLE 8. Reconnaissance SHRIMP I U-Pb dating, Weldborough area zircons, NE Tasmania.

Grain/locality	Colour	Spot	$^{206}Pb/^{238}U$ $\pm 2\sigma$	U	Th	Pb*	%C ^{206}Pb	Age$\pm 2\sigma$
A1. Thomas Plain,	white	1	0.03611 ± 324	47	14	1	12.5	229 ± 20
Weldborough	(clear)	2	0.03898 ± 384	25	7	1	14.1	247 ± 24
D1. Gray's Hill	yellow	1	0.04605 ± 404	46	17	2	12.0	290 ± 25
Branxholm Creek	brown	1	0.02287 ± 206	73	20	1	20.3	146 ± 13

Analyst: P.D. Kinny

TABLE 9. Representative analyses, Weldborough basalts, NE Tasmania.

Analysis:	Main element oxides and CIPW norms (wt.%)										Trace elements (ppm)		
Sample:	BAS and norm			AOB and norm			HAW and norm				BAS	AOB	HAW
SiO_2	44.58	or	7.7	43.36	or	8.9	48.32	or	15.5	Ni	343	147	111
TiO_3	1.99	ab	13.9	2.62	ab	17.3	1.63	ab	28.8	Cr	465	248	243
Al_2O_3	13.91	an	21.8	14.71	an	23.8	16.04	an	18.2	Sc	27	24	16
Fe_2O_3	2.42	ne	5.8	2.61	ne	4.4	2.06	ne	4.6	V	193	176	126
FeO	8.71	di	18.4	9.39	di	14.6	7.41	di	9.9	Ba	326	551	538
MnO	0.18	ol	23.5	0.19	ol	19.7	0.20	ol	14.9	Sr	633	1240	1135
MgO	11.97	il	3.9	8.81	il	5.2	5.95	il	3.2	Rb	30	32	64
CaO	9.63	ap	1.5	9.37	ap	2.4	6.85	ap	1.9	Y	24	29	23
Na_2O	2.87			2.89			4.23			Zr	205	237	479
K_2O	1.27			1.45			2.52			Nb	52	68	101
P_2O_5	0.60			0.96			0.75			La	39	51	63
L.O.I	0.96			2.54			3.09			Ce	69	98	113
Total	99.04			98.90			99.05			Nd	31	45	45
$Mg/(Mg+Fe^{2+})$	0.709			0.626			0.587			U	<2	<1.5	2.5
An/(Ab+An)	0.610			0.579			0.387			Th	4.5	4	7.5
D.I. (ΣOr,Ab,Ne)	27.43			30.54			48.84			Pb	2.5	2	4.5
										Zn	85	84	105
										Cu	77	61	49

Fe_2O_3, FeO and CIPW anhydrous norms calculated at $Fe_2O_3/(FeO + Fe_2O_3) = 0.2$
BAS Basanite (average of two analyses)
AOB Alkali olivine basalt
HAW Hawaiite (average of two analyses)
Analysts: P. Robinson and K. McGoldrick

evolution. In contrast, a published Weldborough alkali basalt (AOB II) analysis is strongly depleted in incompatible elements, such as Rb, K and U, although retaining a pronounced positive Nb anomaly. Such depletion/enrichment patterns have been attributed to amphibole-dominant metasomatism within a mantle peridotite melting source (O'Reilly and Zhang, 1995).

Discussion

These two contrasting gem corundum associations from eastern Australia place further constraints on the likely sources for such suites. A magmatic source, based on the corundum growth and geochemistry, applies to the blue, green, yellow Weldborough sapphires and to a subordinate set of similar sapphires in the Barrington field.

TABLE 10. Key element ratios, Weldborough, NE Tasmania and Tasmanian Seamount basalts.

Basalt Type	Zr/Nb	La/Nb	Ba/Nb	Rb/Nb	Ba/Th	Ba/La	La/Y	Ce/Y
Basanite	3.9–4.0	0.7–0.8	6.1–6.4	0.5–0.6	63–84	8.2–8.7	1.6–1.7	2.9–3.0
Alkali basalt I	3.5	0.8	8.1	0.5	138	10.8	1.8	3.4
Hawaiite	4.8	0.6	5.2–5.5	0.6–0.7	59–91	8.3–8.9	2.62–2.9	4.9–5.0
Alkali basalt II	3.6	0.5	5.2	0.4	82	9.7	0.9	1.9
Seamount basalts	3.1–4.7	0.5–0.7	5.0–7.2	0.3–0.8	64–99	9.0–13		

Alkali basalt II from Sutherland *et al*. (2004*b*); Tasmanian seamounts from Lanyon *et al*. (1993), Crawford *et al*. (1997)

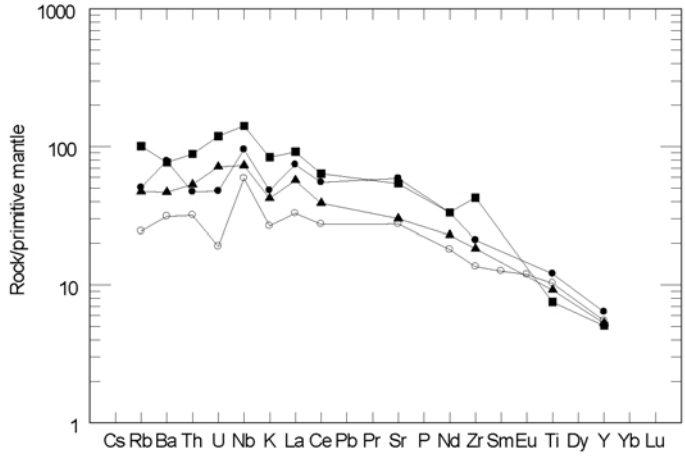

FIG. 6. Multi-element plot of incompatible elements, normalized to primitive mantle values after Sun and McDonough (1989), Weldborough-Gray's Hill basalts (average values from Table 9). Basanite (solid triangles), alkali basalt I (solid circles), hawaiite (solid squares). Alkali basalt II (open circles) from Sutherland *et al.* (2004*a*).

Various proposals for crystallizing corundums from salic melts have invoked evolved, aluminous silicate melts, either giving direct corundum crystallization or *via* a desilification process where more silicic melts interact with less silicic hosts. The evolved melts may be undersaturated (e.g. phonolite/nephline syenite; Irving, 1986), intermediate (e.g. trachyte/syenite; Upton *et al*., 1999), or intermediate, and contaminated with alkaline fluids (Garnier *et al.*, 2005), but are unlikely to be highly silicic due to the propensity of corundum to react with silica (Bottrill, 1998). Examples of corundum-bearing desilicated intrusions ('plumasites') appear in a range of ultramafic to granulitic basements (Garnier *et al*., 2004). Other mechanisms for crystallizing corundum from melts include small-volume felsic melting within metasomatized (amphibole-bearing) mantle, either directly, or indirectly through the fractionation of basaltic melts (Sutherland *et al*., 1998*b*), or by hybrid interactions of carbonatitic melts with silicic crustal intrusives (Guo *et al*., 1996).

Other factors to consider involve temperature, pressure, fluid activity and oxidation effects, e.g. mantle or crustal conditions. Some direct magmatic examples are known, such as a primary sapphire-bearing, mantle-derived monzonite dyke in Precambrian gneisses and migmatites at Dusi, Kenya (Simonet *et al*., 2004) and Cretaceous corundum (+ zircon)-bearing albitite dykes within uplifted mantle peridotites in the French Pyrenees (Monchoux *et al*., 2006; Pin *et al*., 2006). Thus, characterizations of magmatic corundum-bearing assemblages, now disaggregated, partly resorbed and transported by later basaltic events, not only require detailed appraisals of the corundum and zircon xenocrysts, but also the host basalt sources and their geological and geochronological settings.

Weldborough sapphire source

The Ga levels in the Weldborough sapphires (104−520 ppm) typify those reached in extreme end states of alkali magma fractionation (Siedner, 1965). The decrease in Fe and Ti contents from core to rim in most of the sapphires reflects reduced accommodation for these elements in the structure as temperatures fell during growth and/or progressive depletion of these elements in the crystallizing melt. Recent studies (Sampinpanya *et al*., 2003; Wathanakul *et al*., 2004) show that cores of some sapphires from basalt fields contain greater than expected amounts of Be (up to 367 ppm), Nb (up to 2845 ppm), Ta (up to 820 ppm) and Sn (up to 225 ppm), which may have a local source significance. Significant levels of Sn appear in some eastern Australian sapphires (800−1500 ppm) and rubies (600−5300 ppm) (G. Webb, pers. comm., 2004). Potential enrichments of such elements in Weldborough and Barrington corundums also need assessment. Additional analyses of the Weldborough sapphire

cores that included Be, Nb, Ta and Sn (Appendix 1) indicates that Be is negligible (<5 ppm), but Nb (15–57 ppm), Ta (50–157 ppm) and Sn (48–259 ppm) are slightly elevated in several samples. The elevated Sn may be significant as the granite at Weldborough is a tin-bearing type (McClenaghan *et al*., 1982). The only data available for Barrington corundums show minimal Nb and Ta (<10 ppm; M. Garland data, pers. comm., 1998).

During crystallization, the Weldborough sapphires grew from a parental medium enriched in Cl, Fe, Ga, Ti and CO_2, but relatively low in K. The fluid-bearing melt, however, was buffered under relatively reduced lithological conditions, based on the $\delta^{18}O$ isotope values for the sapphires (4.6–6.0‰), which span typical values for ultramafic rocks. This raises the prospect that the sapphire-bearing melts crystallized at mantle levels, particularly as higher-level ultramafic intrusive bodies are not noted in northeastern Tasmania, even in airborne geophysical surveys (Gunn *et al*., 1996).

The mantle lies at ~30 km depth under Weldborough (Rawlinson *et al*., 2001), which equates to ~0.9–1.0 GPa and 900–950ºC for the Tasmanian palaeogeotherm (Sutherland *et al*., 2005). The Weldborough basalts include mantle-derived spinel lherzolite xenoliths, which enhance the potential for corundum transport from such levels. The mantle-derived basalts include partly evolved types, implying fractionation at mantle pressures. The Weldborough hawaiite composition can be achieved from the Weldborough primary basanite, using a least-squares fractional crystallization model (Morris, 1984). This computer modelling suggests crystallization of 3–6% olivine (Fo_{89}), 27–36% clinopyroxene ($Di_{44}En_{54}Fs_2$), 5–6% plagioclase ($Ab_{56-65}An_{26-38}Or_{7-9}$), 5–6% spinel, 5–6% ulvospinel and 1% apatite provides a good-fit solution (squared residuals 0.02–0.05). Such mineral phases are observed as xenocrysts and phenocrysts in the basalts, and there is no evidence that basalt fractionation proceeded to highly evolved felsic end-members. Restricted Late-Cretaceous phonolites and K-rich lamprophyric intrusives occur in northeastern Tasmania (Everard *et al*., 2004), but the low K concentration in fluid inclusions in Weldborough sapphires does not favour links with the Cretaceous melts. The lack of nepheline as an observed inclusion in Weldborough sapphires, as found in some eastern Australian sapphires (Sutherland *et al*., 2003*a*), also counts against a phonolitic melt origin.

The zircon megacrysts that accompany the Weldborough sapphires may provide chronological clues to the crystallization of sapphire. The zircons show magmatic growth features and although their fission track ages are mostly reset by basaltic transport (~47 Ma), their U-Pb ages suggest largely Triassic crystallization ages (208–247±11 Ma). This Mesozoic age range coincides with known but limited eastern Tasmanian basaltic to felsic volcanism, which includes strongly evolved sodic basalt (St Marys basalt ~235 Ma). Thus, the Weldborough sapphires may be coeval with and in part relate to underlying Mesozoic alkaline sources that produced abundant zircons. Recent U-Pb isotope dating on a geochemically distinct zircon megacryst and on a zircon inclusion in sapphire here, however, gave ages near 47 Ma (Brendan McGee and authors' unpublished data), so that at least some sapphires seem linked to the Early Cenozoic basalt event.

Barrington sapphire sources

The higher-Ga sapphire suite at Barrington resembles the Weldborough suite, but is intrinsically richer in Fe and poorer in Ti. Thus, Fe_2O_3/TiO_2 ratios (9–94, av. 25) trend towards higher values than for the Weldborough sapphires (>1, av. 7) and imply that more Fe-rich felsic melts crystallized the Barrington sapphires. Mineral inclusions in these sapphires (anorthoclase, hercynite, spinel, ilmenorutile) also typify intermediate alkaline silicate melt associations. The oxygen isotope values for Weldborough sapphires suggest parental melts buffered by ultramafic rocks, possible in the mantle. It is less clear at Barrington, however, where sapphires give similar values, whether this represents mantle interactions, as higher-level ultramafic bodies also occur nearby. The mantle lithosphere below Barrington, however, clearly contains amphibole-bearing lithologies that can potentially produce corundum-normative felsic melts (Sutherland *et al*., 1998*b*). Zircon megacrysts at Barrington show magmatic growth features and although their fission track ages are reset by basalt transport events, their U-Pb formation ages cluster at 50–60 Ma and 45–46 Ma (Sutherland and Fanning, 2001). Thus, magmatic sapphire and zircon formation below the Barrington field was closely related to the Palaeogene basaltic magmatism.

Weldborough/Barrington sapphire models

Both magmatic sapphire suites come from a similar range of alkali basalts, primary to moderately evolved in nature, with some coming directly from the mantle, or showing trace element imprints, characteristic of amphibole-enriched mantle. The overlap in oxygen isotope values suggests that both sets of sapphires crystallized from melts under similar lithological conditions. They have smaller O isotope values than magmatic sapphires derived from melts contaminated with lower crustal fluids (Garnier *et al.*, 2005). Genetic models which involve siliceous crustal components, e.g. the hybrid carbonatitic/granitic model (Guo *et al.*, 1996), appear inappropriate for the Weldborough/Barrington sapphire O isotope ranges.

Metamorphic corundum sources

The lower-Ga, higher-Cr Barrington suite contrasts with magmatic, higher-Ga sapphire suites, in colour range, spectral properties, mineral association and geochemistry. Greater contents of the Cr chromophore lead to greater Cr_2O_3/Ga_2O_3 ratios (7−150), while the lower Ga contents typify metamorphic corundums (usually <100 ppm) and generally provide Cr_2O_3/Ga_2O_3 ratios that exceed 1 (Saminpanya *et al.*, 2003). Peucat *et al.* (2005) further suggest that metamorphic blue corundums are distinguished in Fe *vs.* Ga/Mg plots, but this discriminator is not applied here as the metamorphic blue sapphires at Barrington are clearly separated from the magmatic blue sapphires by their Cr_2O_3/Ga_2O_3 ratios.

Although metamorphic in character, the Barrington ruby suite presents some unusual genetic features. The fluid/melt inclusions suggest CO_2 was not significant in the crystallizing process, but the glassy, K- and Cl-rich feldspathic silicate melt inclusions imply that some felsic melt interactions took place within the metamorphic setting. Oxygen isotopic compositions of these corundums have relatively low values similar to the magmatic sapphires from Barrington and Weldborough, which were attributed to crystallization within ultramafic mantle (?) rocks. The $\delta^{18}O$ range (5.1−6.2‰) is much less than for most rubies from shear zones, pegmatitic and marble deposits (>7.5−12.3‰), but extends into ranges for rubies from mafic and ultramafic lithologies (2.9−7.5‰); see ranges given by Giuliani *et al*. (2005).

Temperature estimates for Barrington ruby assemblages range between 780 and 940ºC (Sutherland and Coenraads, 1996), but the pressures of crystallization are unconstrained. These temperatures approach those expected for crust-mantle boundary conditions here (O'Neil *et al*., 2003), based on the known Moho depth (>37 km) and its likely intersection with southeastern Australian palaeogeotherms (>930ºC; Sutherland *et al.,* 2005). Barrington rubies, however, do not need mantle depths to account for their O isotope ranges, as ultramafic bodies thrust into the fold belt here provide a suitable higher-level alternative. Intimate associations of high *P-T* sapphirine-bearing assemblages (800−700ºC, 0.6−0.9 GPa) at contacts with uplifted mantle bodies are described in the French Pyrenean massif (Monchoux, 1972), so that similar sources may exist below Barrington Plateau. The ruby-bearing zones may mark ultramafic contacts where interacting alkaline melts liberated Cr-bearing fluids into the system.

This study confirms that the Barrington ruby suite differs from other ruby suites in New South Wales (Sutherland *et al*., 2003, 2004*a*). This spinel-sapphirine-ruby facies contrasts with a higher-*T*, Al-rich diopside-garnet-ruby facies in the Cudgegong-Macquarie River area and a magmatic-related ruby suite in the New England area. It closely resembles a spinel-sapphirine-ruby facies suite from western Palin, Cambodia, even in its oxygen isotope values (Giuliani *et al*., 2005), but clearly differs from garnet-sapphirine-ruby suites from a proposed garnet granulite facies in Thailand (Sutthirat *et al*., 2001).

Conclusions

The Weldborough and Barrington gem corundum comparisons demonstrate several features, both broad- and fine-scale in nature:

(1) The separate magmatic and mixed-magmatic/metamorphic corundum suites yield similar oxygen isotope ranges, regardless of differences in origin. Thus, the crystallizing conditions were probably buffered by ultramafic bodies of different settings, as described by Giuliani *et al.* (2005) and Garnier *et al.* (2005).

(2) Magmatic sapphire/zircon suites and metamorphic corundum suites may originate at quite different times to the basaltic magmatism that disaggregated the gem sources.

(3) Magmatic sapphire suites from different fields can exhibit distinct local differences in their trace-element chemistry.

(4) Sapphire and ruby suites from basaltic belts document a wide variety of corundum-bearing sources that become tapped by basaltic melts.

Acknowledgements

Van Dieman Mines Pty Ltd and Mineral Holdings Australia Pty Ltd were instrumental in providing samples of the Weldborough sapphires and basalts. Dr Mary Garland, then at the University of Toronto, Canada, kindly permitted use of the Barrington corundum trace element results from the PIXE facility at Guelph University, Canada. Dr Gaston Giuliani, CRPG/CNRS, Vandœuvre-les-Nancy, France, and Prof. Anthony Fallick, SNERC, Glasgow, Scotland, provided oxygen isotope results for the Barrington corundums. Dr P.D. Kinny, then at the Research School of Earth Sciences, Australian National University, gave permission to use unpublished SHRIMP I U-Pb results. Gayle Webb, Ross Pogson and Sue Folwell, of the Department of Mineralogy & Petrology, Australian Museum, Sydney, assisted with data, calculations of basalt norms and fractional crystallization testing, and script preparation. The first author thanks Brendan McGee for discussion of the subject. Special thanks are due to David Belton of CSIRO for his patience and help with the analysis and processing of the PIXE data. The Australian Museum Trust and UTas Institutional Research Grant Scheme (IRGS) provided funds for Khin Zaw to investigate the Barrington corundum and north-east Tasmanian sapphire fluid/melt inclusions and for LA ICP-MS analysis of the Tasmanian sapphire samples. Constructive reviews of the manuscript were carried out by Drs Daniel Ohnenstetter, CRPG/CNRS, Vandœuvre, France, and Andrew Christy, DEMS, Australian National University, Canberra.

References

Bottrill, R.S. (1996) *Corundum and Sapphire in Tasmania*. Tasmanian Geological Survey, Record 1996/05 (unpublished).

Bottrill, R.S. (1998) A corundum-quartz assemblage in altered volcanic rocks, Bond Range, Tasmania. *Mineralogical Magazine*, **62**, 325–332.

Campbell, J.L. and Czamanske, G.K. (1998) Micro-PIXE in Earth science. Pp. 169–185 in: *Particle-Induced X-ray Emission Spectrometry* (S.A.E. Johansson, J.L. Campbell and K.G. Malmqvist, editors). Chemical Analysis Series, **133**, Wiley, New York.

Coenraads, R.R., Sutherland, F.L. and Kinny, P.D. (1990) The origin of sapphires: U-Pb dating of zircon inclusions sheds new light. *Mineralogical Magazine*, **54**, 113–122.

Coldham, T. (2003) The history and importance of heat treatment of Australian sapphire. *The Australian Gemmologist*, **21**, 50–62.

Crawford, A.J., Lanyon, R., Elmes, M. and Eggins, S. (1997) Geochemistry and significance of basaltic rocks dredged from the South Tasman Rise and adjacent seamounts. *Australian Journal of Earth Sciences*, **44**, 621–632.

Everard, J.L., Sutherland, F.L. and Zwingmann, H. (2004) A Cretaceous phonolite from the Tomahawk River, Northeast Tasmania. *Papers and Proceedings of the Royal Society of Tasmania*, **138,** 11–33.

Garnier, V., Giuliani, G., Ohnenstetter, D. and Schwarz, D. (2004) Les gizements de corindon: classification et genese. Les placers a corindon gemme. *Le Regne Mineral*, **55**, 7–47.

Garnier, V., Ohnenstetter, D., Giuliani, G., Fallick, A.E., Phan Trong, T., Hoang Quang, L., Pham Van, L. and Schwarz, D. (2005) Basalt petrology, zircon ages and sapphire genesis from Dak Nong, southern Vietnam. *Mineralogical Magazine*, **69**, 21–38.

Giuliani, G., Fallick, A.E., Garnier, V., France-Lanord, C., Ohnenstetter, D. and Schwarz, D. (2005) Oxygen isotope compositions as a tracer for the origins of rubies and sapphires. *Geology*, **33**, 249–252.

Gunn, P.J., Mitchell, J.N. and Meixner, T.J. (1996) The structure and evolution of the Bass and Durroon Basins as delineated by aeromagnetic data. *Australian Geological Survey Organisation Record*, 1996/14 (unpublished).

Guo, J.F., O'Reilly, S.Y. and Griffin, W.L. (1996) Corundum from basaltic terrains: a mineral inclusion approach to the enigma. *Contributions to Mineralogy and Petrology*, **122**, 368–386.

Irving, A.J. (1986) Polybasic magma mixing in alkali basalts and kimberlites: Evidence for corundum, zircon and ilmenite megacrysts. *Geological Society of Australia Abstracts Series*, **16**, 262–264.

Lanyon, R., Varne, R. and Crawford, A.J. (1993) Tasmanian Tertiary basalts, the Balleny Plume, and opening of the Tasman Sea (southwest Pacific Ocean). *Geology*, **21**, 555–558.

Limtrakun, P., Khin Zaw, Ryan, C.G. and Mernagh, J.P. (2001) Formation of the Denchai gem sapphires, northern Thailand: evidence from mineral chemistry and fluid/melt inclusion characteristics. *Mineralogical Magazine*, **65**, 725–735.

Maxwell, J.A., Teesdale, W.J. and Campbell, J.L. (1995) The Geulph PIXE software package II. *Nuclear Instruments and Methods in Physics Research*, **B95**, 407–421.

McClenaghan, M.P., Turner, N.J., Baillie, P.W., Brown,

A.V., Williams, P.R. and Moore, W.R. (1982) Geology of the Ringarooma-Boobyalla area. *Tasmanian Department of Mines*, *Bulletin of the Geological Survey of Tasmania*, **9**, 198 pp.

Monchoux, P. (1972) Roches à sapphirine au contract des lherzolites pyrénéennes. *Contributions to Mineralogy and Petrology*, **37**, 47–64.

Monchoux, P., Fontan, F., Parseval, P. de, Martin, R.F. and Wang, R.C. (2006) Igneous albititic dikes in orogenic lherzolites, Western Pyrenees, France: a possible source for corundum and alkali feldspar xenocrysts in basaltic terranes. I. Mineral Associations. *The Canadian Mineralogist*, **44**, 817–842.

Moore, W.R. (1991) Geology-Winnaleah 1:100, 000. Tasmanian Department of Resources and Energy, Hobart.

Morris, P.A. (1984) MAGFRAC: A basic program for least-squares approximation of fractionational crystallisation. *Computers and Geoscience*, **19**, 437–444.

Oakes, G.M., Barron, L.M. and Lishmund, S.R. (1996) Alkali basalts and associated volcaniclastic rocks as a source of sapphire in eastern Australia. *Australian Journal of Earth Science*, **43**, 289–298.

O'Neil, C., Moresi, L., Lenardic, A. and Cooper, C.M. (2003) Inferences on Australia's heat flow and thermal structure from mantle convection modelling results. *Geological Society of Australia Special Publication*, **22**, and *Geological Society of America Special Paper*, **372**, 169–184.

O'Reilly, S.Y. and Zhang, M. (1995) Geochemical characteristics of lava-field basalts from eastern Australia and inferred sources: connections with the sub-continental lithospheric mantle. *Contributions to Mineralogy and Petrology*, **121**, 148–170.

Peucat, J.J., Ruffault, P., Fritsch, E., Simonet, C., Bouhnik-Le, C. and Lasnier, B. (2005) Un nouvel outil géochimique de reconnaissance des saphirs bleus basaltiques et metamorphiques: Le rapport Ga/Mg. *Revue de Gemmologie*, **152**, 1–5.

Pin, C., Monchoux, P., Paquette, J.-L., Azambre, B., Wang, P.C. and Martin, R.F. (2006) Igneous albititic dikes in orogenic lherzolites, Western Pyrenees, France: a possible source for corundum and alkali feldspar xenocrysts in basalt terranes. II. Geochemical and petrogenetic considerations. *The Canadian Mineralogist*, **44**, 843–856.

Rawlinson, N., Houseman, G.A., Collins, C.D.N. and Drummond, B.J. (2001) New evidence of Tasmania's tectonic history from a novel seismic experiment. *Geophysical Research Letters*, **28,** 3337–3340.

Roberts, D.L., Sutherland, F.L., Hollis, J.D., Kennewell, P. and Graham, I.T. (2004) Gemstone characteristics, North-East Barrington Plateau, NSW. *Journal & Proceedings of the Royal Society of New South Wales*, **137**, 99–122.

Ryan, C.G., Heinrick, C.A., van Achterbergh, E., Balhaus, C. and Mernagh, T.P. (1995) Microanalysis of ore-forming fluids using the scanning proton microprobe. *Nuclear Instrument Method*, **B104**, 182–190.

Ryan, C.G., van Achterbergh, E., Yeates, C., Drieberg, S.L., Mark, G., McInnes, B.M., Win, T.T. and Suter, G.F. (2002) Quantitative, high sensitive, high resolution, nuclear microprobe imaging of fluids, melts and minerals. *Nuclear Instrument Method*, **B188**, 18–27.

Saminpanya, S., Manning, D.A.C., Droop, G.T.R. and Henderson, C.M.B. (2003) Trace elements in Thai gem corundums. *Journal of Gemmology*, **28**, 392–398.

Sharp, Z.D. (1990) A laser-based microanalytical method for the in situ determination of oxygen isotope ratios of silicates and oxides. *Geochimica et Cosmochimica Acta*, **54**, 1353–1357.

Siedner, G. (1965) Geochemical features of a strongly fractionated alkali igneous suite. *Geochimica et Cosmochimica Acta*, **29**, 113–137.

Simonet, C., Paquette, J.L., Pin, C., Lasnier, B. and Fritsch, E. (2004) The Dusi (Garba Tula) sapphire deposit, Central Kenya – a unique Pan-African corundum-bearing monzonite, *Journal of African Earth Sciences*, **38**, 401–410.

Sun, S.-S. and McDonough, W.F. (1989) Chemical and isotopic systematics of oceanic basalts: implications for mantle composition and processes. Pp. 313–345 in: *Magmatism in the Ocean Basins.* Special Publication, **42**, Geological Society, London.

Sutherland, F.L. (1996) Alkaline rocks and gemstones, Australia: a review and synthesis. *Australian Journal of Earth Sciences*, **43**, 323–343.

Sutherland, F.L. and Coenraads, R.R. (1996) An unusual ruby-sapphirine-spinel assemblage from the Tertiary Barrington volcanic province, New South Wales. *Mineraogical Magagazine*, **60**, 623–638.

Sutherland, F.L. and Fanning, C.M. (2001) Gem-bearing basaltic volcanism, Barrington New South Wales: Cenozoic evolution based on basalt K-Ar ages and zircon fission track and U-Pb isotope dating. *Australian Journal of Earth Sciences*, **48**, 221–237.

Sutherland, F.L. and Graham, I.T. (2003) *Geology of the Barrington Tops Plateau. Its Rocks, Minerals and Gemstones, New South Wales, Australia.* The Australian Museum Society, Sydney, 56 pp.

Sutherland, F.L. and Schwarz, D. (2001) Origin of gem corundums from basaltic fields. *The Australian Gemmologist*, **21**, 30–33.

Sutherland, F.L. and Wellman, P. (1986) Potassium-argon ages of Tertiary volcanic rocks, Tasmania.

Papers and Proceedings of the Royal Society of Tasmania, **120**, 77–86.

Sutherland, F.L., Schwarz, D., Jobbins, E.A., Coenraads, R.R. and Webb, G. (1998*a*) Distinctive gem corundum suites from discrete basalt fields: a comparative study of Barrington, Australia and West Pailin, Cambodia, gemfields. *Journal of Gemmology*, **26**, 65–85.

Sutherland, F.L., Hoskin, P.W.O., Fanning, C.M. and Coenraads, R.R. (1998*b*) Models of corundum origin from alkali basalt terrains: A reappraisal. *Contributions to Mineralogy and Petrology*, **133**, 356–72.

Sutherland, F.L., Graham, I.T., Pogson, R.E., Schwarz, D., Webb, G.B., Coenraads, R.R., Fanning, C.M., Hollis, J.D. and Allen T.C. (2002*a*) The Tumbarumba basaltic gem field, New South Wales: In relation to sapphire-ruby deposits of eastern Australia. *Records of the Australian Museum*, **54**, 215–248.

Sutherland, F.L., Bosshart, G., Fanning, C.M., Hoskin, P.W.O. and Coenraads R.R. (2002*b*) Sapphire crystallisation age and origin, Ban Huai Sai, Laos: age based on zircon inclusions. *Journal of Asian Earth Sciences*, **20**, 841–849.

Sutherland, F.L., Coenraads, R.R., Schwarz, D., Raynor, L.R., Barron, B.J. and Webb, G.B. (2003) Al-rich diopside in alluvial ruby and corundum-bearing-bearing xenoliths, Australian and SE Asian basalt fields. *Mineralogical Magazine*, **67**, 717–732.

Sutherland, F.L., Graham, I.T. and Webb, G.B. (2004*a*) Sapphire-ruby-zircon deposits from basaltic fields, West Pacific continental margins. Pp. 385–387 in: *Metallogeny of the Pacific Northwest: Tectonics, Magmatism and Metallogeny of Active Continental Margins* (A.I. Khanchuk, G.A. Gonevechuk, A.N. Mitrokhin, L.F. Simanenko, N.J. Cook and R. Seltmann, editors). Dalnauka, Vladivostok, Russia.

Sutherland, F.L., Graham, I.T., Everard, J.L. Forsyth, S.M. and Zwingmann, H. (2004b) *Cenozoic basalts, Tasmania: Landscapes, exposures, ages, petrography, geochemistry, entrainments and petrogenesis.* Field Guide A5. 17th Australian Geological Convention, Hobart, Tasmania, Geological Society of Australia, 58 pp.

Sutherland, F.L., Raynor, L.R. and Pogson, R.E. (2005) Table Cape vent xenolith suite, N.W. Tasmania: Mineralogy and implications for crust-mantle lithology and Miocene geotherms in Tasmania. *Papers and Proceedings of the Royal Society of Tasmania*, **139**, 7–22.

Sutthirat, C., Saminpanya, S., Droop, G.T.R., Henderson, C.M.B. and Manning, D.A.C. (2001) Clinopyroxene-corundum assemblages from alkali-basalt and alluvium, eastern Thailand: constraints on the origin of Thai rubies. *Mineralogical Magazine*, **65**, 277–295.

Upton, B.G.J., Hinton, R.W., Aspen, P., Finch, A. and Valley, J.W. (1999) Megacrysts and associated xenoliths: evidence for migration of geochemical enriched melts in the upper mantle beneath Scotland. *Journal of Petrology*, **40**, 935–956.

Veevers, J.J. (2001) *ATLAS of Billion-year earth history of Australia and neighbours in Gondwanaland.* GEMOC PRESS, Sydney, 76 pp.

Vysotskii, S.V., Shcheka, S.A., Nechaev, V.P., Soroka, V.P., Barkov, A.V. and Khanchuk, A.I. (2002) First finding of sapphire from Cenozoic alkali-basaltic volcanoes in the Primor'e region. *Doklady Akademi Nauk CCP*, *Earth Science*, **387A**, 1100–1103.

Wathanakul, P., Atitchat, W., Pisutha-Arnond, V., Win, Tin Tin and Singbamroong, S. (2004) Evidence on the unusually high Be, Sn, Nb and Ta content in some trapiche-like sapphires from basaltic origins. *29th International Gemmological Conference, Wuhan, China. Abstracts*, 114–117.

Yim, W.W.-S., Gleadow, A.J.W. and Van Moort, J.C. (1985) Fission track dating of alluvial zircons and heavy mineral provenance in North-east Tasmania. *Journal of the Geological Society of London*, **142**, 351–356.

Yui, Tzen-Fu, Khin Zaw and Limtraken, P. (2003) Oxygen isotope compositions of the Denchai sapphires, Thailand: A clue to their enigmatic origin. *Lithos*, **67**, 153–161.

[*Manuscript received 20 December 2005: revised 15 December 2006*]

APPENDIX I. Additional trace element LA ICP-MS analysis (ppm) of sapphires from NE Tasmania.

Grain (analysis)	Fe range	Ti range	Ga Range	V	Cr	Be	Nb	Ta	Sn
NET 1c(2)	2734–3349	355–421	267–283	4.9–6.6	< 0.6	0.1–4.9	0.2–4.1	1.6–157	2.2–4.1
NET 2c(2)	2253–2446	197–428	112–115	1.8–1.9	0.6–1.1	0.1	0.4–0.5	2.5–3.0	3.4–7.5
NET 3c(2)	3265–3608	2024–2432	201–208	7.8–9.6	0.6–0.9	2.9–3.4	46–57	109–132	120–121
NET 4c(2)	2607–3201	174–193	162–179	11–13	0.6–3.0	0.1	1.1–1.6	0.7	0.5–1.5
NET 5c(2)	3698–4334	75–82	134–155	1.7–2.1	0.4–0.7	0.0–0.1	0.0–0.4	0.8	3.3–3.7
NET 6c(2)	1834–2302	243–252	152–158	0.6–1.1	0.7–1.0	1.1–1.4	15–22	51–57	48–259
NET 7c(2)	2543–3012	417–423	198–218	1.4–1.6	0.4–1.0	1.8–2.2	15–19	63–50	134–139
NET 8c(2)	2129–2412	101–114	198–204	1.0	<0.5	0.2–0.3	0.3–0.4	8.7–9.3	38–41
NET 9c(2)	2821–2965	14–21	202–241	2.4–3.2	4.0–25	0.3–1.5	1.2–4.1	12–56	2.4–4.3

Analyses represent two analyses of the central area of each grain. The results are standardized against an Al content of 529,200 ppm for corundum.
LA ICP-MS analyst: S. Gilbert.
Detection limit-ranges (DL, ppm), with analytical precisions if > DL (% 1 st. dev), for these elements are:
Fe (2.11–3.62), ±1.7–2.1; Ti (0.22–0.61), ±1.8–3.9; Ga (0.02–0.04) ±1.4–3.2; V (0.02–0.03), ±1.7–4.8;
Cr (0.34–0.57), ±2.6–35.8; Be (0.01–0.02), ±2.8–20.7; Nb (0.01–0.02), ±1.8–30.4; Ta (0.00–0.01), ±1.5–11.0;
Sn (0.03–0.05), ±1.5–15.1.